

---

# Action Draft and Verify: A Self-Verifying Framework for Vision-Language-Action Model

---

Chen Zhao<sup>†12</sup> Zhuoran Wang<sup>12</sup> Haoyang Li<sup>†12</sup> Shifeng Bao<sup>†3</sup> Guanlin Li<sup>†12</sup> Youhe Feng<sup>†1</sup> Yang Li<sup>12</sup>  
Jie Tang<sup>4</sup> Jing Zhang<sup>12</sup>

## Abstract

Vision-Language-Action (VLA) models have recently demonstrated strong performance across embodied tasks. Modern VLAs commonly employ diffusion action experts to efficiently generate high-precision continuous action chunks, while auto-regressive generation can be slower and less accurate at low-level control. Yet auto-regressive paradigms still provide complementary priors that can improve robustness and generalization in out-of-distribution environments. To leverage both paradigms, we propose Action-Draft-and-Verify (ADV): diffusion action expert drafts multiple candidate action chunks, and the VLM selects one by scoring all candidates in a single forward pass with a perplexity-style metric. Under matched backbones, training data, and action-chunk length, ADV improves success rate by +4.3 points in simulation and +19.7 points in real-world over diffusion-based baseline, with a single-pass VLM reranking overhead.

## 1. Introduction

Recent VLA models often couple a Vision-Language Model (VLM) backbone with a diffusion action expert, which preserves the semantic understanding capabilities of VLMs while leveraging the high-precision action characteristic of diffusion models. It has been adopted by a series of pre-trained VLAs such as  $\pi_0$  (Black et al., 2025a) and GR00T (Bjorck et al., 2025), demonstrating promising performance across both simulated and real-world environments.

However, this design can introduce failure modes under distribution shift. Diffusion-based VLAs predict continuous actions solely conditioned on feature representations extracted

<sup>†</sup>Done as intern at Zhipu AI. <sup>1</sup>School of Information, Renmin University of China <sup>2</sup>Key Laboratory of Data Engineering and Knowledge Engineering, Beijing, China <sup>3</sup>Beijing University of Posts and Telecommunications <sup>4</sup>Tsinghua University. Correspondence to: Jing Zhang <zhang-jing@ruc.edu.cn>.

Table 1. Evaluation results on RoboTwin2.0 (partial) benchmarks.

RoboTwin2.0 (partial)	Diffusion		Auto-Regression	
	Easy	Hard	Easy	Hard
Avg. Success Steps ( $\downarrow$ )	292.0	449.6	<b>286.3</b>	<b>334.5</b>
Recovery Attempts ( $\uparrow$ )*	4.5	0.4	<b>6.2</b>	<b>9.2</b>
Env. Collision Before First Grasp (% , $\downarrow$ ) <sup>†</sup>	<b>0</b>	29.7	<b>0</b>	<b>2.3</b>
Avg. Success Rate (%)	<b>57.7</b>	<b>15.0</b>	33.3	3.7

\* The average number of attempts after the first failure.

<sup>†</sup> The probability that the target is collided and deviates from the arm’s action space due to random jittering of the gripper before first attempt.

by the VLM. When facing out-of-distribution (OOD) environments, diffusion-based VLA models tend to exhibit underfitting behaviors such as reduced recovery attempts and increased jitter collisions, as they may underutilize pre-trained VLM priors for structured generalization to the same extent as auto-regressive VLA models (Liu et al., 2025). Furthermore, due to the stochastic nature of diffusion inference (Feng et al., 2025), action execution becomes less deterministic, which may lead to suboptimal trajectories even under identical test conditions.

To examine the aforementioned issues, we conduct experiments on three RoboTwin2.0 tasks (Table 1)<sup>1</sup>. We compare a Qwen2.5-VL-3B (Bai et al., 2025) model augmented with a diffusion action expert against an auto-regressive baseline in which the same VLM generates action chunks of the same length. Both methods are evaluated under matched training data and backbone initialization. Although diffusion achieves higher success rates in both in-distribution (RoboTwin2.0 Easy) and OOD (RoboTwin2.0 Hard) evaluations, the auto-regressive baseline exhibits more stable corrective behavior under distribution shift, with fewer pre-grasp collisions and more consistent recovery attempts. In OOD environments, the diffusion method becomes less effective at recovery: recovery attempts (the average number of corrective tries after the first failure) drop from 4.5 to 0.4. Meanwhile, pre-grasp jitter increases, raising *Env. Collision Before First Grasp* from 0.0% to 29.7%. The auto-regressive method does not exhibit this behavior. Even in

<sup>1</sup>Evaluation tasks include “adjust bottle”, “block ranking rgb”, and “open laptop”. The complete test results are presented in Table 2 and Table 5.

OOD environments, the auto-regressive baseline maintains its corrective behavior: recovery attempts increase from 6.2 to 9.2, consistent with its in-distribution execution pattern. Consequently, it causes minimal environmental disruption: random jittering increases only slightly (0.0%  $\rightarrow$  2.3%) and remains far lower than the diffusion action expert (29.7%).

To combine the high success rate of diffusion with the superior stability of auto-regressive models under distribution shift, we propose an **Action Draft and Verify (ADV)** framework. Specifically, it includes two stages: In the draft phase, the action expert receives hidden state from the VLM and generates multiple candidate action trajectories. In the verification phase, we score all candidates in parallel with a single VLM forward pass and select the chunk with the lowest length-normalized negative log-likelihood (a perplexity-style score). The verified actions demonstrate superior precision and continuity, with particularly notable improvements in OOD environments. Notably, during verification we use a VLM perplexity-style score for reranking, rather than asking the VLM to generate actions token-by-token. To make likelihood-based verification reliable, we introduce Textual FAST, which renders compressed action codes as text and re-tokenizes them with the pretrained VLM tokenizer, avoiding low-frequency action-only vocabulary items.

We perform a series of validity analyses to understand why using an auto-regressive model as a verifier can improve diffusion-based inference. Although the VLM verification may not always pinpoint the optimal action, it filters out suboptimal action chunks, which serves as the fundamental reason for the framework’s success. In OOD environments, the diffusion model occasionally produces actions that are either ineffective or harmful to the task due to unfamiliar conditions. In ADV, the auto-regressive module identifies and rejects anomalous outputs.

To conclude, the main contributions of this paper are summarized as follows:

- **A lightweight inference framework for diffusion-based VLAs:** We introduce ADV, an action-draft-and-verify inference framework: a diffusion action expert drafts multiple candidate action chunks conditioned on the VLM, and the VLM reranks these candidates via perplexity-style verification to select the final action chunk.
- **Broad Effectiveness Across Models:** We show that ADV can be applied to a diverse set of VLMs and pre-trained VLAs—including Qwen2.5-VL (Bai et al., 2025), InternVL3.5 (Wang et al., 2025b), and  $\pi_{0.5}$  (Black et al., 2025a)—and improves performance in both simulation and real-world evaluations over diffusion-based and auto-regressive baselines under matched settings.
- **Mechanistic Insights into Model Robustness:** We analyze why ADV improves robustness under distribution

shift. Results indicate that VLM-based verification primarily acts as a failure-mode filter—rejecting low-quality or erroneous action chunks—rather than relying on perfectly identifying the single optimal candidate, which leads to more reliable VLA execution.

## 2. Related Work

**Auto-regressive VLA and diffusion-based VLA.** Current VLA frameworks primarily fall into two categories: auto-regressive models and diffusion models (Brohan et al., 2022; Shao et al., 2025). Diffusion-based VLAs can generate continuous actions with high precision and temporal smoothness (Ze et al., 2024; Liu et al., 2024; Team et al., 2024; Black et al., 2025b). In contrast, directly using a VLM to predict actions as tokens can better leverage the pre-trained knowledge embedded in VLMs than decoding actions through diffusion action expert (Zitkovich et al., 2023; Wang et al., 2024; Li et al., 2025). Spec-VLA (Wang et al., 2025a) adds draft model to accelerate action generation. Although the draft–verify idea is similar to ours, it is fundamentally different: their goal is to improve the inference efficiency of auto-regressive models, whereas ours aims to combine the strengths of auto-regression and diffusion.

Recent work has explored hybrid approaches that combine diffusion and auto-regression to further improve VLA performance. At the training stage,  $\pi_{0.5}$  (Black et al., 2025a) and G0 (Jiang et al., 2025) co-train a VLM to output discrete action tokens alongside a diffusion action expert for continuous action, partially preserving VLM capabilities while improving overall performance. At inference time, Hybrid-VLA fuses diffusion and auto-regressive action predictions, achieving state-of-the-art performance on RL Bench (James et al., 2020). However, forced weighted-averaging fusion can be sensitive under OOD shift: when the two predictors disagree, averaging may produce an intermediate trajectory that is less plausible than either constituent prediction. Instead of blending predictions, we formulate inference as *selection*: a diffusion expert proposes multiple candidate action chunks, and the VLM *verifies* them by scoring and selecting a single candidate. More broadly, ADV follows a *decoding-as-selection* paradigm: it generates multiple candidates and then selects one via model-based scoring, akin to reranking in LLM decoding (Wang et al., 2022; Nakano et al., 2022) and best-of-N selection with learned or pre-trained scorers (Ouyang et al., 2022; Radford et al., 2021).

**Discrete Action Tokens.** Auto-regressive VLA models typically represent actions as discrete tokens (Wang et al., 2025a; Chopra et al., 2025). These tokens are often mapped to low-frequency entries in the VLM vocabulary or introduced via an auxiliary vocabulary, and inference proceeds token-by-token (e.g., generating a 7-DoF pose

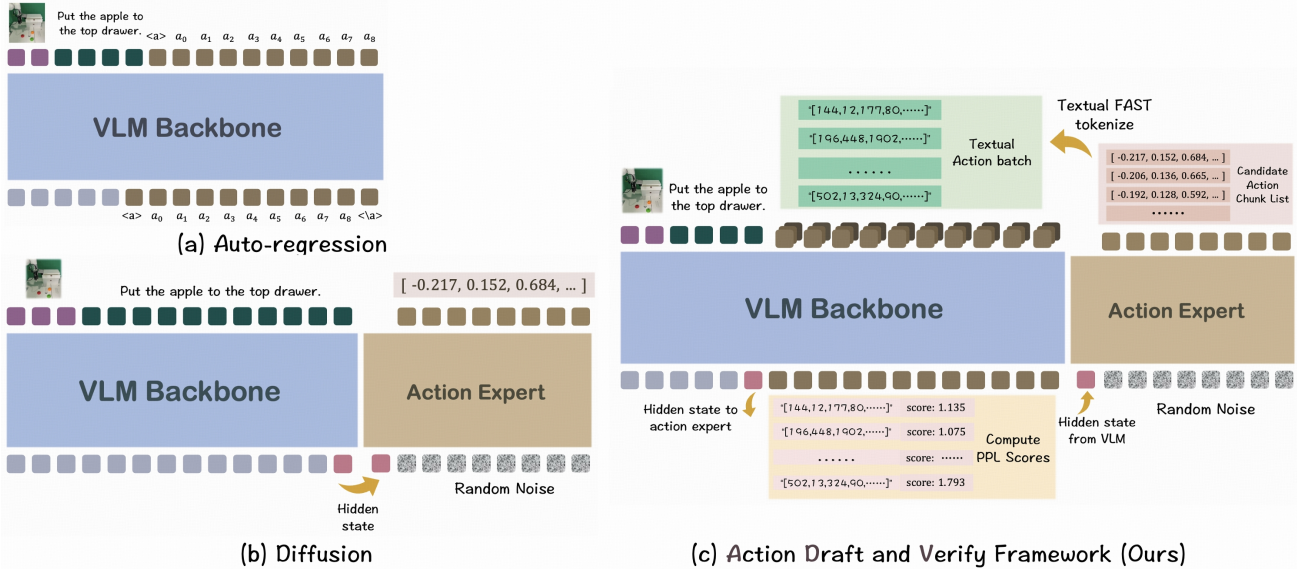


Figure 1. Overview Inference Framework (a) **Auto-regression-based** VLA models generate actions via token-by-token decoding. (b) **diffusion-based** VLA models predict continuous actions using an additional action expert conditioned on feature representations extracted by the VLM. (c) **Ours**: In the draft phase, the action expert takes the VLM hidden states as input and generates multiple candidate action trajectories. In the verification phase, the VLM scores all candidates in a single forward pass and selects the trajectory with the best (lowest) perplexity-style score as the final output.

$[x, y, z, \text{roll}, \text{pitch}, \text{yaw}, \text{gripper}]$  by predicting seven tokens sequentially) (Zitkovich et al., 2023). FAST (Pertsch et al., 2025) compresses action sequences using discrete cosine transform and byte pair encoding to speed up decoding and improve performance. VLA-0 (Goyal et al., 2025) instead maps actions into text-like representations that better match the VLM pre-training distribution, substantially accelerating training. We combine FAST-style efficiency with VLA-0’s text-aligned representations to design our tokenization, enabling more stable VLM-based scoring in ADV.

### 3. Method

ADV applies to VLAs that couple an auto-regressive VLM backbone with a diffusion action expert. In this section, we describe the training objective, the **draft-and-verify** inference procedure, and **Textual FAST**, a discrete action-token representation tailored for stable VLM-based scoring.

#### 3.1. Notation and Training

We adopt a VLM + diffusion action expert architecture (Figure 1(c)). At each decision step, the diffusion action expert proposes a set of candidate action chunks  $S = \{A_0, \dots, A_{M-1}\}$ . Each chunk  $A_n = \langle a_0, \dots, a_{H-1} \rangle$  is a sequence of continuous actions of size  $H$ , where  $a_k$  is the action at timestep  $k$  (a 7-DoF end-effector action (position,

orientation, and gripper command) for each gripper)<sup>2</sup>.

For auto-regressive modeling and for verification, we convert each action chunk into a token sequence using Textual FAST (Section 3.3):  $\tilde{A}_n \mapsto \langle t_0, \dots, t_{T_n-1} \rangle$ , where  $t_i$  is the  $i$ -th token and  $T_n$  is the resulting token length.

**Auto-regressive objective.** Given instruction  $\ell$  and observation  $o$ , standard auto-regressive training minimizes the negative log-likelihood (NLL) of the target action tokens:

$$\mathcal{L}_{\text{VLM}}(\theta) = \mathbb{E}_{(o, \ell, \tilde{A}) \sim \mathcal{D}} \left[ - \sum_{i=0}^{T-1} \log \pi_{\theta}(t_i \mid o, \ell, t_{<i}) \right]. \quad (1)$$

**Diffusion objective.** The VLM produces a final-layer hidden feature  $f_c$  that conditions the diffusion action expert. We train the diffusion expert with a flow-matching loss over timestamps  $\tau \in [0, 1]$ :

$$\mathcal{L}_{\text{dif}}(\theta, \phi) = \mathbb{E}_{(o, \ell, A) \sim \mathcal{D}, \epsilon, \tau} \left[ \left\| \pi_{\phi}(A^{\tau}, f_c, \tau) - (A - \epsilon) \right\|^2 \right], \quad (2)$$

where  $A^{\tau} = \tau A + (1 - \tau)\epsilon$  is the noisy action at time  $\tau$  (Lipman et al., 2022) and  $\epsilon \sim \mathcal{N}(0, I)$  is Gaussian noise. Here  $\theta$  and  $\phi$  denote the parameters of the VLM backbone and the diffusion action expert, respectively. The flow-matching

<sup>2</sup>For bimanual control, we define  $a_k$  as the concatenation of the two grippers’ 7-DoF poses.

loss backpropagates through  $f_c$ , and thus optimizes both  $\theta$  and  $\phi$ .

**Co-training.** In practice, the auto-regressive component typically converges faster than the diffusion expert; the VLM backbone may overfit before the diffusion expert reaches its best performance. To better synchronize optimization, we weight the diffusion loss with a factor  $\beta$ :

$$\mathcal{L}_{\text{co-train}}(\theta, \phi) = \mathcal{L}_{\text{VLM}}(\theta) + \beta \mathcal{L}_{\text{dif}}(\theta, \phi). \quad (3)$$

### 3.2. Draft and Verify

**Draft.** Conditioned on the VLM hidden feature  $f_c$ , the diffusion action expert samples multiple candidate chunks by varying the injected noise, yielding  $S = \{A_0, \dots, A_{M-1}\}$ . These candidates represent diverse, plausible trajectories. Because the diffusion expert is lightweight and uses only a few denoising steps (Table 10), the drafting overhead is typically small relative to a single VLM forward pass<sup>3</sup>.

**Verify.** We score all candidates in parallel in one batched VLM forward pass by computing their teacher-forced log-likelihoods conditioned on the same observation and instruction. Since candidates are tokenized using Textual FAST (Section 3.3), the token length  $T_n$  may vary across candidates. For efficient batching, we pad each candidate’s action-token sequence to a fixed maximum length of 2048. We then compute a length-normalized perplexity-style score:

$$C_{A_n} = \exp\left(-\frac{1}{T_n} \sum_{t_i \in \bar{A}_n} \log \pi_{\theta}(t_i | o, \ell, t_{<i})\right). \quad (4)$$

We select the final action chunk by

$$A^* = \arg \min_{A_n \in S} C_{A_n}. \quad (5)$$

This verification step lets the VLM reject low-quality candidates while retaining the diffusion expert’s high-precision continuous control.

### 3.3. Discrete Action Tokenization

We propose **Textual FAST**, a discrete action tokenization method that combines the efficiency of FAST (Pertsch et al., 2025) with the text-aligned representation idea of VLA-0 (Goyal et al., 2025). Textual FAST first encodes action chunks into compact discrete tokens using the FAST tokenizer. It then renders these tokens as text and re-tokenizes them with the standard VLM tokenizer.

<sup>3</sup>With our default setting (4 denoising steps and  $M = 16$  candidates), drafting is inexpensive relative to a single VLM forward pass.

Textual FAST provides two benefits: (i) FAST-style compression captures temporal structure and motion range efficiently; and (ii) representing actions as text avoids introducing new, low-frequency vocabulary items and better matches the VLM pre-training distribution, improving the reliability of likelihood-based verification. Because Textual FAST re-tokenizes the rendered text, it often yields longer token sequences than FAST alone after re-tokenization with the VLM tokenizer. However, ADV verification uses a single forward pass for scoring (rather than token-by-token decoding), so this increased token length does not require token-by-token auto-regressive decoding; it only affects the cost of the single scoring forward pass. See Appendix A and Figure 3 for illustrations of the different tokenization schemes.

## 4. Experiment

This section provides a comprehensive evaluation of our framework in both simulated and real-world environments. Our experiments are specifically designed to address four key research questions:

**Q1: ADV Performance.** How does ADV perform compared to auto-regressive and diffusion-based baselines?

**Q2: ADV Mechanism Analysis.** What are the underlying factors driving ADV’s efficacy in both in-distribution and out-of-distribution (OOD) environments?

**Q3: Scoring Reliability.** How effective is the perplexity-style score as a metric for filtering low-quality actions during verification?

**Q4: Tokenization Impact.** How does Textual FAST compare to other tokenization schemes in the context of discrete action verification?

**Setup.** To assess the impact of each component, we define the following configurations based on the model types:

- **VLM-based models:** We compare three variants: (1) Model-FAST, which auto-regressively generates discrete action tokens using the FAST tokenizer; (2) Model-Diffusion, which augments the VLM with a diffusion action expert for continuous action generation; and (3) Model-ADV, which is co-trained with both auto-regressive and diffusion objectives and uses the proposed ADV draft-and-verify procedure at inference time. We evaluate two backbones: Qwen2.5-VL-3B and InternVL3.5-2B. See Appendix B.1 for action expert parameters.
- **VLA-based models:** We adopt the state-of-the-art VLA model  $\pi_{0.5}$ . To enable ADV on  $\pi_{0.5}$ , we co-train it using the same combined auto-regressive and diffusion objectives. At inference time, we use the original diffusion-based decoding for  $\pi_{0.5}$ , and the proposed ADV inference procedure for  $\pi_{0.5}$ -ADV.

Table 2. **Main benchmark results for ADV and baselines.** “Model-FAST”: FAST tokenizer-assisted auto-regression model. “Model-Diffusion”: a VLM augmented with a diffusion action expert. “Model-ADV”: model incorporating VLM verification into model-Diffusion. Qwen2.5-VL-FAST was evaluated on a subset of tasks within RoboTwin2.0. Detailed training settings are provided in Table 11.

Benchmark	Model	Action Chunk	Steps per Second	Success Rate (%)						
				Spatial	Object	Goal	Long	Avg.		
<b>LIBERO</b>										
	Qwen2.5-VL-FAST	16	5.0hz	90.2	88.6	96.2	76.4	87.9		
	Qwen2.5-VL-Diffusion	16	68.4hz	94.6	97.2	93.8	90.2	93.9		
	<b>Qwen2.5-VL-ADV (Ours)</b>	16	41.0hz	96.6	<u>98.8</u>	97.0	94.6	96.8		
	InternVL3.5-FAST	16	3.2hz	89.6	92.8	93.6	82.8	89.6		
	InternVL3.5-Diffusion	16	57.6hz	95.8	96.0	94.2	92.8	94.7		
	<b>InternVL3.5-ADV (Ours)</b>	16	36.9hz	97.6	<b>99.4</b>	<u>97.2</u>	<u>96.8</u>	<u>97.8</u>		
	$\pi_{0.5}$	16	61.6hz	<u>97.8</u>	98.4	96.6	93.0	96.5		
	<b><math>\pi_{0.5}</math>-ADV (Ours)</b>	16	37.3hz	<b>98.4</b>	<b>99.4</b>	<b>98.2</b>	<b>97.6</b>	<b>98.4</b>		
<b>RoboTwin 2.0</b>				<b>Adjust Bottle</b>	<b>Open Laptop</b>	<b>Block Rank RGB</b>	<b>.....</b>	<b>Avg.</b>		
	Qwen2.5-VL-FAST	32	6.9hz	Easy   Hard	Easy   Hard	Easy   Hard	0.0	Easy   Hard		
	Qwen2.5-VL-Diffusion	32	94.7hz	53.0   6.0	34.0   5.0	13.0   0.0	...	-   -		
	<b>Qwen2.5-VL-ADV (Ours)</b>	32	53.3hz	96.0   16.0	39.0   18.0	38.0   11.0	...	30.1   6.7		
				<b>97.0   26.0</b>	<b>55.0   27.0</b>	<b>52.0   24.0</b>	...	<b>39.3   10.2</b>		
<b>Real-World</b>				<b>Push Blocks</b>	<b>Clean Table</b>	<b>Pick &amp; Place</b>	<b>Hang Cups</b>	<b>Avg.</b>		
	Qwen2.5-VL-FAST	5	3.3hz	38.5	36.7	41.3	19.5	34.5		
	Qwen2.5-VL-Diffusion	5	26.1hz	56.2	52.5	45.5	43.7	49.5		
	<b>Qwen2.5-VL-ADV (Ours)</b>	5	14.4hz	<u>75.4</u>	<b>72.5</b>	75.0	62.5	71.4		
	InternVL3.5-FAST	5	3.0hz	31.2	29.5	46.5	35.3	35.7		
	InternVL3.5-Diffusion	5	20.9hz	54.1	56.7	55.0	68.7	58.6		
	<b>InternVL3.5-ADV (Ours)</b>	5	12.5hz	72.7	66.7	<b>83.3</b>	<b>81.3</b>	<u>76.1</u>		
	$\pi_{0.5}$	5	24.6hz	74.0	61.5	71.3	55.3	65.6		
	<b><math>\pi_{0.5}</math>-ADV (Ours)</b>	5	15.8hz	<b>81.7</b>	<u>70.7</u>	<u>79.5</u>	<u>78.3</u>	<b>77.6</b>		

Our simulation experiments are conducted on LIBERO (Liu et al., 2023) and RoboTwin2.0 (Chen et al., 2025). For real-world evaluation, we design four tasks: targeted blocks pushing, table cleaning with a drawer, instruction-based pick-and-place, and precision cups hanging.

We do not compare HybridVLA’s autoregressive–diffusion combination method because it is built on an MLP-based action expert attached to a VLM, which differs from our setting that uses a diffusion-based action expert. However, we report comparison results with HybridVLA on LIBERO in Table 12.

**Metrics.** We evaluate the success rate using a consistent **Action Chunk** size, defined as the number of low-level control steps executed per policy query (i.e., per VLA inference). To evaluate efficiency, we report **Steps per Second (Hz)**, defined as the action chunk size divided by the end-to-end inference latency per chunk (including candidate drafting, VLM scoring, and post-processing). To detail performance, we introduce three additional metrics. **Avg. Success Steps** is the average steps in successful trajectories, where lower values indicate more decisive task completion. **Recovery Attempts** is the average number of recovery attempts after the first failure (e.g., re-grasping or re-approaching). Higher counts suggest a better capability to recover from execution failures. **Env. Collision Before First Grasp** measures the probability that the target is accidentally collided with and displaced due to gripper jitter before the first grasp attempt. Lower values indicate more stable and precise grasping. For

real-world tasks, we report a normalized task completion score converted to Success Rate (%) as described in Appendix B.3. Unless otherwise specified, all methods use the same action chunk length per benchmark, and ADV uses  $M = 16$  candidates with 4 denoising steps (Table 10). See Appendix B for experimental setting details.

#### 4.1. Main Results

In this section, we evaluate the performance gains from ADV across multiple benchmarks to assess its overall effectiveness for robotic task execution.

**Experiment Settings.** We train Qwen2.5-VL, InternVL3.5, and  $\pi_{0.5}$  on the LIBERO, RoboTwin2.0, and real-world datasets. For RoboTwin2.0, we follow the official setting by training only on the Easy dataset. Due to the limited evaluation throughput, we do not test the performance of InternVL3.5 and  $\pi_{0.5}$  on RoboTwin2.0.

**Results.** As shown in Table 2, our method outperforms all baselines under identical settings. On LIBERO, ADV improves success rate by +2.9 percentage points on Qwen2.5-VL, +3.1 points on InternVL3.5, and +1.9 points on  $\pi_{0.5}$  over diffusion-based inference, averaging a +2.7-point gain. On RoboTwin2.0, ADV improves success rate by +9.2 points on Easy tasks and +3.5 points on Hard tasks compared to diffusion-based inference. In real-world environments, compared to diffusion-based inference, ADV improves success rate by +21.9 points on Qwen2.5-VL, +17.5

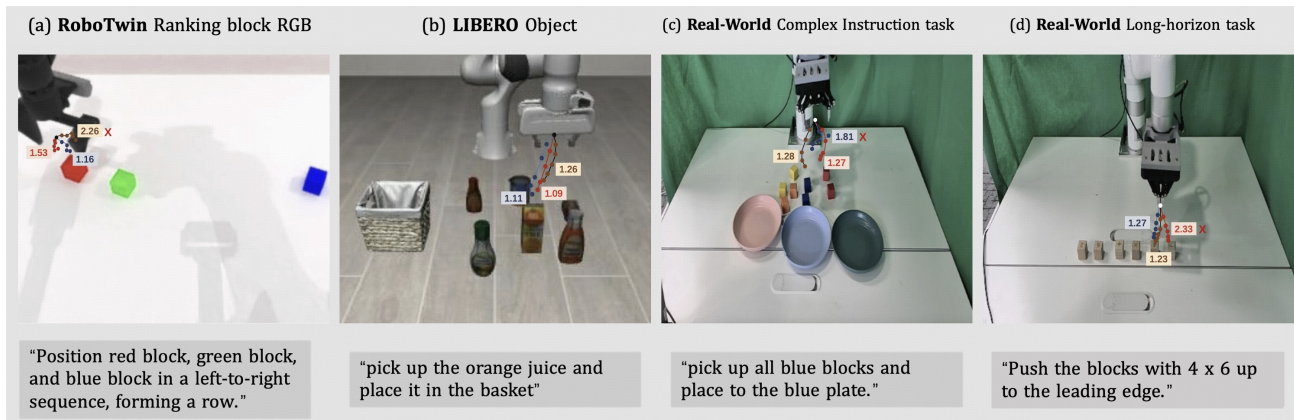


Figure 2. **Examples of confidence scoring for action trajectories across all benchmark environments.** While the VLM verifier sometimes fails to select the most precise action (b-red&b-blue; d-blue&d-brown), it effectively filters out actions that are evidently erroneous (d-red) or insufficiently direct (a-brown, c-blue).

Table 3. Impact of Selecting the X-th Ranked Action by Perplexity-Style Score on Success Rate on LIBERO-Long.

Choose K-th Action	K=1	K=2	K=3	K=4	K=5	K=6	...	K=15	K=16	Random
Success Rate (%)	<u>94.6</u>	<b>94.8</b>	94.2	91.6	89.0	87.4	...	87.6	88.2	90.2

points on InternVL3.5, and +12.0 points on  $\pi_{0.5}$ , with a +17.1-point improvement on average. Notably, ADV consistently improves performance for both general VLMs without embodied pre-training and VLAs with embodied pre-training. With ADV, general VLMs achieve performance comparable to several strong pre-trained VLAs (Tables 12 and 13).

While ADV introduces additional inference overhead compared to diffusion-based inference, it maintains a high control rate (steps per second; Table 2), ensuring smooth and responsive robot motions. Moreover, in OOD environments, ADV often completes tasks in fewer steps (Avg. Success Steps; Table 5) than diffusion-based baselines, keeping the overall execution time largely unchanged.

## 4.2. ADV Mechanism Analysis

In this part, we evaluate ADV in both in-distribution and OOD settings to investigate the mechanisms underlying its effectiveness in seen and unseen environments.

**Experiment Settings.** We evaluate the ADV framework through four sets of experiments. The basic configurations are as follows:

- **K-th Best Experiment.** We measure the success rate on LIBERO-Long using Qwen2.5-VL-ADV by selecting the action chunk with the K-th lowest perplexity (Eq. (4)) from a candidate set of 16, instead of selecting the lowest-perplexity chunk. "Random" corresponds to uniformly

sampling one candidate from the diffusion drafts, matching the Qwen2.5-VL-Diffusion inference setting.

- **Real-World Generalization.** We assess performance on unseen instructions and objects in real-world environments; detailed settings are provided in Appendix C.
- **RoboTwin2.0 (Hard).** We evaluate success rate and three auxiliary metrics: Avg. Success Steps, Recovery Attempts, and Env. Collision Before First Grasp.
- **Recovery Capability Experiment.** In the real-world "push blocks" task, we use a two-stage strategy: we first execute several chunks inferred by the diffusion-based model with a longer action chunk length (32 steps), and then switch to a shorter chunk length (5 steps) to evaluate recovery with and without ADV.

**Results.** These experiments address the following question: although diffusion is often more sample-efficient and precise for low-level continuous control than auto-regressive decoding, why can VLM-based verification still improve diffusion-based inference? Our analysis suggests that VLM verification helps maintain correct trajectories by rejecting suboptimal draft actions, thereby improving the effectiveness of the diffusion action expert.

**Discarding the bad rather than finding the single best.** To understand the role of VLM verification, we analyze performance when selecting the K-th best action chunk according to Eq. (4) (Table 3). Among top-ranked chunks, the

Table 4. Success rate evaluated on the Real-World (Unseen) environment (%).

Real-World (Unseen)	Push Blocks	Clean Table	Pick & Place	Hang Cups	Avg.
Qwen2.5-VL-Diffusion	5.0	8.0	28.0	32.0	18.3
<b>Qwen2.5-VL-ADV (Ours)</b>	<b>45.0</b>	24.0	36.0	40.0	<b>36.3 (+18.0)</b>
InternVL3.5-Diffusion	10.0	8.0	16.0	40.0	18.5
<b>InternVL3.5-ADV (Ours)</b>	40.0	16.0	32.0	<b>56.0</b>	<b>36.0 (+17.5)</b>
$\pi_{0.5}$	25.0	16.0	<b>40.0</b>	40.0	30.3
<b><math>\pi_{0.5}</math>-ADV (Ours)</b>	40.0	<b>48.0</b>	<b>40.0</b>	48.0	<b>44.0 (+13.7)</b>

Table 5. Evaluation results on RoboTwin2.0 (Hard). ( $\pm k$ ) indicates the change in the metric relative to the diffusion-based baseline.

RoboTwin2.0 (Hard)	Adjust Bottle			Blocks Ranking RGB			Open Laptop			Shake Bottle		
	ADV	Diffusion	FAST	ADV	Diffusion	FAST	ADV	Diffusion	FAST	ADV	Diffusion	FAST
Avg. Success Steps ( $\downarrow$ )	<b>107.3 (-45.2)</b>	152.5	84.3	<b>754.0 (-282.9)</b>	1036.9	-	<b>142.3 (-17.1)</b>	159.4	99.6	<b>95.3 (-54.4)</b>	149.7	104.2
Recovery Attempts ( $\uparrow$ )	<b>1.1 (+0.7)</b>	0.4	8.5	<b>3.3 (+2.6)</b>	0.7	14.1	<b>2.9 (+2.6)</b>	0.3	3.5	<b>1.3 (+0.6)</b>	0.7	10.9
Env. Collision Before First Grasp (% , $\downarrow$ )	<b>3 (-43)</b>	46	0	<b>14 (-15)</b>	29	5	<b>0 (-14)</b>	14	2	<b>4 (-34)</b>	38	0
Success Rate (% , $\uparrow$ )	<b>26 (+10)</b>	16	6	<b>24 (+13)</b>	11	0	<b>27 (+9)</b>	18	5	<b>37 (+16)</b>	21	13

Table 6. Recovery capability evaluation of ADV (%). On real-world push block task, perform 32 steps per chunk for several action chunks by InternVL3.5-Diffusion, then switch to 5 steps per chunk to test recovery capability from low quality prefix actions.

Number of Long Chunks*	$\infty$	2	1	0
InternVL3.5-Diffusion	17.0	17.0	33.0	100.0
<b>InternVL3.5-ADV (Ours)</b>	17.0	<b>33.0</b>	<b>83.0</b>	100.0

\* The count of consecutive inferences using the 32 steps per chunk (long chunk) before switching back to 5 steps per chunk.

success rate changes only marginally; however, the success rate drops sharply when the rank reaches  $K \geq 4$ . This indicates that the VLM backbone is not always able to identify the globally optimal action chunk, but it is effective at filtering out poor ones. As shown in Figure 2, ADV selects an action chunk that is neither a “destroyer” (d-red) nor a “slacker” (a-brown, c-blue). In this sense, the verifier acts as a trajectory keeper, keeping diffusion-generated trajectories on track toward task completion.

### Trajectory keeping in out-of-distribution environments.

We evaluate ADV on four RoboTwin2.0 tasks and in unseen real-world environments. In real-world evaluation (Table 4), ADV shows strong generalization, improving success rate by +16.4 points on average over diffusion-based baselines. In the RoboTwin2.0 (Hard) (Table 5), ADV increases the average success rate by +12.0 points across four tasks. Compared to diffusion-based inference, ADV reduces Avg. Success Steps by 99.9, increases Recovery Attempts by 1.6, and reduces Env. Collision Before First Grasp by 26.5 points on average across the four tasks. Because RoboTwin2.0 (Hard) is fully OOD, arm motions can appear chaotic and unstable. With ADV verification, the robot is more proactive in re-grasping after failures and causes less environmental distur-

bance due to random jitter—a common failure mode when grasping under unseen conditions. These improvements lead to faster completion and higher overall reliability.

### Fault rescue within in-distribution environments.

OOD conditions can also emerge in in-distribution settings due to the state sensitivity of VLA action prediction: small errors may push the system into rarely seen states, where diffusion becomes unstable. To amplify prediction errors and stress recovery, we increase the action chunk length from 5 to 32 steps (about 6.4 seconds) for several chunks, and then switch back to 5-step chunks. We evaluate recovery with and without ADV under these induced OOD states (Table 6). With two long chunks—covering about two-thirds of the task—ADV shows a clear recovery advantage (33% vs. 17%). When limited to one long chunk (about one-third of the task), ADV successfully completes nearly the entire task (83% vs. 33%). These results suggest that when imprecise predictions lead to unfamiliar states, ADV can steer the system back onto the correct trajectory, as long as the robot has not caused irreversible changes to the environment.

In summary, ADV improves VLA policies in two key ways:

- (i) it filters out low-quality or erroneous actions, reducing failures caused by poor action chunks; and
- (ii) it enables robust error recovery, allowing verified action chunks to keep the system on a correct trajectory even under OOD conditions, thereby improving overall robustness.

### 4.3. VLM Verification Effectiveness Analysis

In this part, we analyze the relationship between the perplexity-style score and task success to assess whether Eq. (4) provides a reliable metric for filtering candidate actions during verification.

**Experiment Settings.** To evaluate whether VLM perplexity

Table 7. Avg. perplexity-style score of successful trajectories and failed trajectories on LIBERO. The trajectories are generated by Qwen2.5-VL-Diffusion, and scored using the perplexity-style score defined in Eq. (4).

LIBERO	Spatial	Object	Goal	Long	Avg.
Avg. Score in Fail (↓)	1.707	1.637	2.196	2.901	2.110
Avg. Score in Success (↓)	1.338	1.242	1.549	1.729	1.465
<b>Success Rate (%)</b>	94.6	97.2	93.8	90.2	93.9

Table 8. Impact of noise on success rate on LIBERO.

Noise Range	Noise=0.1%	Noise=1%	Noise=3%	Noise=10%
Avg. Chosen Rate (% , ↑)*	12.6	69.7	89.4	99.6
Success Rate (% , ↑)	93.2	89.6	85.4	91.2

\* In each set of action chunks, one is left without adding noise. This is the selection rate for the single noise-free action in each set of action chunks.

can be used for verification, we conduct two experiments:

- **Group Analysis by Outcome.** We split trajectories generated by Qwen2.5-VL-Diffusion on LIBERO into successful and failed groups, and compute the average verification score for each group.
- **Noise Robustness Experiment.** On LIBERO, we inject random action noise into all candidate action chunks in the candidate set  $S$  except the first chunk  $A_0$ . We then measure the task success rate and how often the verifier selects the noise-free chunk  $A_0$ .

**Results.** Our evaluation shows that the perplexity-style verification score is a key component of ADV for filtering imprecise actions. As shown in Table 7, successful trajectories have substantially lower scores than failed ones. Moreover, lower scores correlate with higher task success, consistent with the selection rule  $\arg \min_{A_n \in S} C_{A_n}$  in Eq. (5).

In the noise-robustness experiment (Table 8), larger noise magnitudes make the clean action chunk easier to distinguish. As injected noise increases, the probability of selecting the noise-free chunk  $A_0$  (Avg. Chosen Rate) also rises. This suggests that ADV can detect and reject noisy candidates, mitigating their impact on task execution. Regardless of the noise level, using the proposed VLM verifier to select among candidates helps avoid corrupted trajectories and improves the likelihood of executing a successful one.

#### 4.4. Textual FAST Tokenization Analysis

We compare Textual FAST with alternative action tokenization schemes to examine how action representation affects ADV verification.

**Experiment Settings.** We evaluate different action representations by replacing Textual FAST with several tokenization

Table 9. Impact of tokenization methods (%).

LIBERO	Spatial	Object	Goal	Long	Avg.
Qwen2.5-VL-Diffusion	94.6	97.2	93.8	90.2	93.9
Action Bins	92.8	95.6	94.4	89.0	93.0 ↓
FAST	95.0	97.2	93.6	91.8	94.4 ↑
VLA-0	<b>96.8</b>	<b>95.4</b>	<b>96.0</b>	<b>91.4</b>	<b>94.9 ↑</b>
<b>Textual FAST</b>	<b>96.6</b>	<b>98.8</b>	<b>97.0</b>	<b>94.6</b>	<b>96.8 ↑</b>

baselines while keeping Qwen2.5-VL-3B fixed as the backbone. The baselines are: (1) **Action Bins** (discretize each action dimension into a fixed number of bins, e.g., OpenVLA), (2) **FAST** (compress actions with DCT followed by BPE tokenization, e.g.,  $\pi_0$ -FAST), and (3) **VLA-0** (convert discretized action bins into plain text). We compare these variants by success rate on LIBERO.

**Results.** As shown in Table 9, Textual FAST improves success rate by +2.4 and +1.9 percentage points over FAST and VLA-0, respectively. We attribute the gains to two factors. First, text-rendered action representations are better aligned with the VLM pre-training distribution, making perplexity-style scoring more reliable. Second, efficient action compression reduces verification noise from repetitive and redundant tokens. Notably, directly discretizing the action space for verification (Action Bins) yields a lower success rate than executing the diffusion expert output without verification (Qwen2.5-VL-Diffusion).

## 5. Conclusion

We propose Action Draft-and-Verify (ADV), where a diffusion action expert drafts multiple candidate action chunks and a VLM selects one via single-pass perplexity-style scoring, improving robustness under distribution shift. ADV works because the VLM verifier reliably filters out anomalous or low-quality drafts, keeping execution on a stable, task-consistent trajectory even when the diffusion sampler is stochastic. Under matched settings, ADV increases success by +4.3 in simulation and +19.7 in real-world with only one-pass reranking overhead.

Despite these gains, ADV has several limitations. First, ADV mainly improves performance on tasks that are already within the capability of the underlying VLA; when the diffusion policy fails to propose any viable candidate action chunk, verification cannot recover a successful trajectory. Second, ADV introduces additional inference latency compared to diffusion-based inference, since it requires drafting multiple candidates and running a batched VLM scoring pass. In practice, this overhead can be reduced with more efficient chunking and execution strategies (e.g., real-time chunking (Black et al., 2025c)), and is often offset by

ADV’s tendency to complete tasks in fewer steps, leaving end-to-end execution time largely unchanged.

## 6. Impact Statement

This paper presents work whose goal is to advance the field of Machine Learning. There are many potential societal consequences of our work, none which we feel must be specifically highlighted here.

## References

- Bai, S., Chen, K., Liu, X., Wang, J., Ge, W., Song, S., Dang, K., Wang, P., Wang, S., Tang, J., et al. Qwen2. 5-vl technical report. *arXiv preprint arXiv:2502.13923*, 2025.
- Bjorck, J., Castañeda, F., Cherniadev, N., Da, X., Ding, R., Fan, L., Fang, Y., Fox, D., Hu, F., Huang, S., et al. Gr00t n1: An open foundation model for generalist humanoid robots. *arXiv preprint arXiv:2503.14734*, 2025.
- Black, K., Brown, N., Darpinian, J., Dhabalia, K., Driess, D., Esmail, A., Equi, M. R., Finn, C., Fusai, N., Galliker, M. Y., et al.  $\pi_{0.5}$ : a vision-language-action model with open-world generalization. In *9th Annual Conference on Robot Learning*, 2025a.
- Black, K., Brown, N., Driess, D., Esmail, A., Equi, M., Finn, C., Fusai, N., Groom, L., Hausman, K., Ichter, B., et al.  $\pi_0$ : A vision-language-action flow model for general robot control. corr, abs/2410.24164, 2024. doi: 10.48550. *arXiv preprint ARXIV.2410.24164*, 2025b.
- Black, K., Galliker, M. Y., and Levine, S. Real-time execution of action chunking flow policies. *arXiv preprint arXiv:2506.07339*, 2025c.
- Brohan, A., Brown, N., Carbajal, J., Chebotar, Y., Dabis, J., Finn, C., Gopalakrishnan, K., Hausman, K., Herzog, A., Hsu, J., et al. Rt-1: Robotics transformer for real-world control at scale. *arXiv preprint arXiv:2212.06817*, 2022.
- Bu, Q., Yang, Y., Cai, J., Gao, S., Ren, G., Yao, M., Luo, P., and Li, H. Univla: Learning to act anywhere with task-centric latent actions. *arXiv preprint arXiv:2505.06111*, 2025.
- Chen, T., Chen, Z., Chen, B., Cai, Z., Liu, Y., Li, Z., Liang, Q., Lin, X., Ge, Y., Gu, Z., et al. Robotwin 2.0: A scalable data generator and benchmark with strong domain randomization for robust bimanual robotic manipulation. *arXiv preprint arXiv:2506.18088*, 2025.
- Chi, C., Feng, S., Du, Y., Xu, Z., Cousineau, E., Burchfiel, B., and Song, S. Diffusion policy: Visuomotor policy learning via action diffusion. In *Proceedings of Robotics: Science and Systems (RSS)*, 2023.
- Chopra, S., McMoil, A., Carnovale, B., Sokolson, E., Kubendran, R., and Dickerson, S. Everydayvla: A vision-language-action model for affordable robotic manipulation. *arXiv preprint arXiv:2511.05397*, 2025.
- Driess, D., Springenberg, J. T., Ichter, B., Yu, L., Li-Bell, A., Pertsch, K., Ren, A. Z., Walke, H., Vuong, Q., Shi, L. X., et al. Knowledge insulating vision-language-action models: Train fast, run fast, generalize better. *arXiv preprint arXiv:2505.23705*, 2025.
- Feng, G., Geng, Y., Guan, J., Wu, W., Wang, L., and He, D. Theoretical benefit and limitation of diffusion language model. *arXiv preprint arXiv:2502.09622*, 2025.
- Goyal, A., Hadfield, H., Yang, X., Blukis, V., and Ramos, F. Vla-0: Building state-of-the-art vlas with zero modification. *arXiv preprint arXiv:2510.13054*, 2025.
- James, S., Ma, Z., Arrojo, D. R., and Davison, A. J. Rlbench: The robot learning benchmark & learning environment. *IEEE Robotics and Automation Letters*, 5(2):3019–3026, 2020.
- Jiang, T., Yuan, T., Liu, Y., Lu, C., Cui, J., Liu, X., Cheng, S., Gao, J., Xu, H., and Zhao, H. Galaxea open-world dataset and g0 dual-system vla model. *arXiv preprint arXiv:2509.00576*, 2025.
- Kim, M. J., Finn, C., and Liang, P. Fine-tuning vision-language-action models: Optimizing speed and success. *arXiv preprint arXiv:2502.19645*, 2025a.
- Kim, M. J., Pertsch, K., Karamcheti, S., Xiao, T., Balakrishna, A., Nair, S., Rafailov, R., Foster, E. P., Sanketi, P. R., Vuong, Q., et al. Openvla: An open-source vision-language-action model. In *Conference on Robot Learning*, pp. 2679–2713. PMLR, 2025b.
- Lee, J., Duan, J., Fang, H., Deng, Y., Liu, S., Li, B., Fang, B., Zhang, J., Wang, Y. R., Lee, S., et al. Molmoact: Action reasoning models that can reason in space. *arXiv preprint arXiv:2508.07917*, 2025.
- Li, H., Chen, Y., Cui, W., Liu, W., Liu, K., Zhou, M., Zhang, Z., and Zhao, D. Survey of vision-language-action models for embodied manipulation. *arXiv preprint arXiv:2508.15201*, 2025.
- Lipman, Y., Chen, R. T., Ben-Hamu, H., Nickel, M., and Le, M. Flow matching for generative modeling. *arXiv preprint arXiv:2210.02747*, 2022.
- Liu, B., Zhu, Y., Gao, C., Feng, Y., Liu, Q., Zhu, Y., and Stone, P. Libero: Benchmarking knowledge transfer for lifelong robot learning. *Advances in Neural Information Processing Systems*, 36:44776–44791, 2023.

- Liu, J., Chen, H., An, P., Liu, Z., Zhang, R., Gu, C., Li, X., Guo, Z., Chen, S., Liu, M., et al. Hybridvla: Collaborative diffusion and autoregression in a unified vision-language-action model. *arXiv preprint arXiv:2503.10631*, 2025.
- Liu, S., Wu, L., Li, B., Tan, H., Chen, H., Wang, Z., Xu, K., Su, H., and Zhu, J. Rdt-1b: a diffusion foundation model for bimanual manipulation. *arXiv preprint arXiv:2410.07864*, 2024.
- Nakano, R., Hilton, J., Balaji, S., Wu, J., Ouyang, L., Kim, C., Hesse, C., Jain, S., Kosaraju, V., Saunders, W., et al. Webgpt: Browser-assisted question-answering with human feedback, 2022. URL <https://arxiv.org/abs/2112.09332>, 2022.
- Ouyang, L., Wu, J., Jiang, X., Almeida, D., Wainwright, C., Mishkin, P., Zhang, C., Agarwal, S., Slama, K., Ray, A., et al. Training language models to follow instructions with human feedback. *Advances in neural information processing systems*, 35:27730–27744, 2022.
- Pertsch, K., Stachowicz, K., Ichter, B., Driess, D., Nair, S., Vuong, Q., Mees, O., Finn, C., and Levine, S. Fast: Efficient action tokenization for vision-language-action models. *arXiv preprint arXiv:2501.09747*, 2025.
- Radford, A., Kim, J. W., Hallacy, C., Ramesh, A., Goh, G., Agarwal, S., Sastry, G., Askell, A., Mishkin, P., Clark, J., et al. Learning transferable visual models from natural language supervision. In *International conference on machine learning*, pp. 8748–8763. PmLR, 2021.
- Shao, R., Li, W., Zhang, L., Zhang, R., Liu, Z., Chen, R., and Nie, L. Large vlm-based vision-language-action models for robotic manipulation: A survey. *arXiv preprint arXiv:2508.13073*, 2025.
- Shukor, M., Aubakirova, D., Capuano, F., Kooijmans, P., Palma, S., Zouitine, A., Aractingi, M., Pascal, C., Russi, M., Marafioti, A., et al. Smolvla: A vision-language-action model for affordable and efficient robotics. *arXiv preprint arXiv:2506.01844*, 2025.
- Team, O. M., Ghosh, D., Walke, H., Pertsch, K., Black, K., Mees, O., Dasari, S., Hejna, J., Kreiman, T., Xu, C., et al. Octo: An open-source generalist robot policy. *arXiv preprint arXiv:2405.12213*, 2024.
- Wang, L., Chen, X., Zhao, J., and He, K. Scaling proprioceptive-visual learning with heterogeneous pre-trained transformers. *Advances in neural information processing systems*, 37:124420–124450, 2024.
- Wang, S., Yu, R., Yuan, Z., Yu, C., Gao, F., Wang, Y., and Wong, D. F. Spec-vla: speculative decoding for vision-language-action models with relaxed acceptance. In *Proceedings of the 2025 Conference on Empirical Methods in Natural Language Processing*, pp. 26916–26928, 2025a.
- Wang, W., Gao, Z., Gu, L., Pu, H., Cui, L., Wei, X., Liu, Z., Jing, L., Ye, S., Shao, J., et al. Internvl3. 5: Advancing open-source multimodal models in versatility, reasoning, and efficiency. *arXiv preprint arXiv:2508.18265*, 2025b.
- Wang, X., Wei, J., Schuurmans, D., Le, Q., Chi, E., Narang, S., Chowdhery, A., and Zhou, D. Self-consistency improves chain of thought reasoning in language models. *arXiv preprint arXiv:2203.11171*, 2022.
- Ze, Y., Zhang, G., Zhang, K., Hu, C., Wang, M., and Xu, H. 3d diffusion policy: Generalizable visuomotor policy learning via simple 3d representations. *arXiv preprint arXiv:2403.03954*, 2024.
- Zhong, Z., Yan, H., Li, J., Liu, X., Gong, X., Zhang, T., Song, W., Chen, J., Zheng, X., Wang, H., et al. Flowvla: Visual chain of thought-based motion reasoning for vision-language-action models. *arXiv preprint arXiv:2508.18269*, 2025.
- Zitkovich, B., Yu, T., Xu, S., Xu, P., Xiao, T., Xia, F., Wu, J., Wohlhart, P., Welker, S., Wahid, A., et al. Rt-2: Vision-language-action models transfer web knowledge to robotic control. In *Conference on Robot Learning*, pp. 2165–2183. PMLR, 2023.

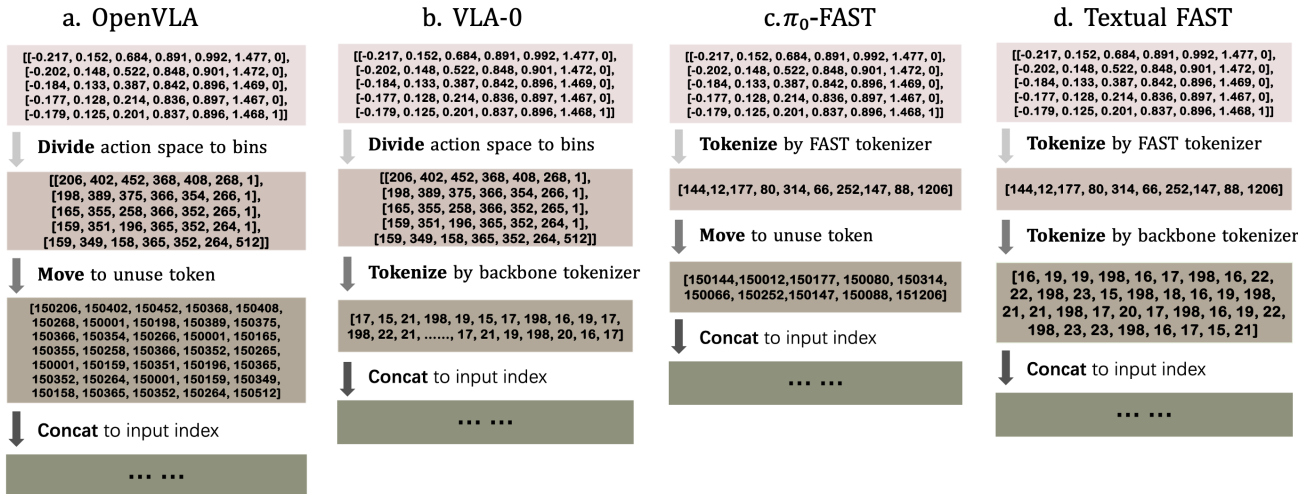


Figure 3. Examples of four discrete action token representation methods. Assume VLM tokenizer encode ‘\n’ to 198, ‘0’ to 14, ‘1’ to 15, ‘2’ to 16 and so on.

## A. Four Action Tokenization Methods

In this section, we illustrate the tokenization differences among four discrete encoding methods, using a concrete example where **action chunk**=5 and **action dim**=7 (see Figure 3).

### A.1. Action Bins

The Action Bins method, adopted by RT-2 and OpenVLA, determines range boundaries using the 1st and 99th percentiles of every dimension of action space and divides each action dimension into 512 bins. Although simple and intuitive, such methods perform poorly when learning dexterous skills with high-frequency control. Highly correlated action tokens diminish the effectiveness of the next token prediction objective used in auto-regressive VLAs. Intuitively, in such cases low token prediction loss can often be achieved with mappings as trivial as simply copying the most recent action token, leaving models in poor local optima (Pertsch et al., 2025).

### A.2. FAST

The FAST tokenizer transforms continuous robot actions into tokens through the following steps:

**Quantile Normalization:** Raw action chunks are normalized such that the 1st and 99th quantiles of the training data map to  $[-1, 1]$ . This ensures robustness to outliers and facilitates cross-embodiment training.

**Discrete Cosine Transform (DCT):** Each action dimension is converted into the frequency domain via DCT, transforming time-series signals into frequency coefficients.

**Quantization:** DCT coefficients are scaled by a hyperparameter  $\gamma$  and rounded to integers. This creates a sparse matrix where high-frequency components often reduce to zero, effectively compressing the signal.

**Flattening:** The sparse coefficient matrix is flattened into a one-dimensional vector of integers using a “column-first” order. By prioritizing low-frequency components across dimensions, this order improves the stability of auto-regressive prediction.

**Byte Pair Encoding (BPE):** The flattened sequence is further compressed into a shorter sequence of dense tokens using a trained BPE tokenizer. This step losslessly merges frequent coefficient combinations and eliminates redundant zero-valued components.

In the introduction to Textual FAST, we refer to this entire process simply as **FAST tokenization**.

### A.3. VLA-0

Common VLM tokens and VLA action tokens often follow distinct distributions, which can lead to interference during the training process. VLA-0 proposes a simple method to circumvent this issue. First, VLA-0 divides each action dimension into several bins. Then, VLA-0 treats the sequence of actions as strings and encodes the action strings using VLM’s tokenizer. In this way, the action sequence is processed similarly to numerical tasks in natural language processing, thereby reducing the

Table 10. Action Expert Model Parameters.

Category	Parameter	Value
<b>Model Size</b>	Number of layers	16
	Hidden size	1536
	Number of attention heads	32
	Parameter size	~500M
<b>Action Config</b>	De-noising step	4
	Number of candidate action chunks $M$	16
<b>Layer Structure</b>	Self-attention layer	All <b>even</b> layers
	Cross-attention layer	All <b>odd</b> layers
	Dropout	0.2
<b>Activation</b>	Activation function	GELU

modality gap. This optimization effectively accelerates convergence speed for VLAs that lack prior pre-training on discrete action tokens.

#### A.4. Textual FAST

Building upon VLA-0, Textual FAST replaces dividing each action dimension into several bins with processing using FAST tokenization. Specifically, Textual FAST first processes actions into action tokens via FAST tokenization, and subsequently treats the sequence of actions as a string and encodes this action string using the VLM’s tokenizer.

## B. Experimental Settings

Experimental settings mainly include the key parameters of the action expert model, training configurations, and the evaluation criteria for real-world experiments.

### B.1. Action Expert Model

Inspired by GROOT-N1, our action expert utilizes an alternating sequence of DiT and self-attention during inference, as detailed in Table 10. To balance training efficiency with strong generalization, we implemented a 16-layer Transformer framework where self-attention and cross-attention layers are interleaved. With a total parameter count of roughly 500M, the model is trained entirely from scratch using random weights for each experiment.

### B.2. Training Settings

Our experiments are primarily conducted on LIBERO, RoboTwin2.0, and in real-world environments. For each benchmark, we use its corresponding dataset to co-train the action expert for continuous actions and the VLM for discrete action tokens. For the evaluation stage, we test the performance of the three inference schemes—auto-regression, diffusion, and the ADV framework—using the same checkpoint. Refer to Table 11 for specific training settings.

### B.3. Real-World Experiment Scoring Details

For each rollout, we record a normalized success rate  $S \in [0, 1]$ , representing the percentage of task completion. This metric accounts for partial completion, which is common in real-world manipulation, and is more informative than binary success indicators. To ensure clarity, we report the success rate as  $\text{Success Rate} = 100\% \times S$  in the main paper, while maintaining  $S \in [0, 1]$  in the appendix tables.

- **Push Blocks:** In the block-pushing task, the total score is comprised of a partial score and a completion score. For

Table 11. Training Configuration on LIBERO, RoboTwin2.0 and Real-world benchmark.

Category	Parameter	Real-World	LIBERO	RoboTwin2.0*
<b>Dataset Statistics</b>	Total episodes	2005	1693	2500
	Total frames	366152	273465	549787
	Task	4	40	50
	Instruction type	741	40	2420
	FPS	5	10	50
<b>Training Parameters</b>	Batch size	144	144	120
	Epoch	32	64	96
	Learning rate	$5 \times 10^{-5}$	$5 \times 10^{-5}$	$2 \times 10^{-5}$
	Weight decay	$1 \times 10^{-5}$	$1 \times 10^{-5}$	$1 \times 10^{-5}$
<b>Other Settings</b>	Seed	42	42	42
	Discrete tokenizer	Textual FAST	Textual FAST	Textual FAST
	Action chunk length $H$	5	16	32
	Co-training loss coefficient $\beta$	3	3	1

\* In actual training, fine-tuning is performed on every single task, consistent with the official settings.

example, in the “push CAT forward” task, pushing the “C”, “A”, and “T” blocks accounts for 25% of the partial score each. The remaining 25% is awarded if all three blocks are successfully pushed and no other blocks are moved. For each block-pushing trial, we assign an individual score  $s \in [0, 1]$  based on the final block configuration, using the following rubric:

- $s = 0.0$ : The current block remains untouched throughout the experiment.
- $s = 0.3$ : The current block is touched but not successfully pushed.
- $s = 0.5$ : The current block is pushed but did not reach the designated finish line.
- $s = 1.0$ : The current block is successfully pushed past the finish line.

We define  $s^r$  as the aggregate score for the  $N$  target blocks in the instructions, and  $s^w$  as the penalty score for the  $M$  unmentioned blocks. Ideally, an optimal trajectory should successfully push all mentioned blocks while leaving the unmentioned blocks untouched, leading to the following scoring criteria:

$$S_{\text{push}} = \frac{1}{N+1} \left( \sum_{i=1}^N s_i^r + 1 - \frac{1}{M} \sum_{i=1}^M s_i^w \right).$$

- **Clean Table:** The table-cleaning task is categorized into three distinct phases: opening the drawer, placing all items (typically three) from the table into the drawer sequentially, and closing the drawer.

We define the score for opening and closing a drawer as binary values,  $s_o, s_c \in \{0, 1\}$ , where 1 indicates the drawer was successfully manipulated, and 0 indicates manipulation failure or no attempt. For each pick-up attempt, we assign an individual nesting score  $s \in [0, 1]$  using the following rubric based on the final block configuration:

- $s = 0.0$ : The current object remains untouched throughout the experiment.
- $s = 0.8$ : The current object is picked up but not successfully placed in the drawer.
- $s = 1.0$ : The current object is successfully picked up and placed in the drawer.

We denote  $s^d$  as the score for the  $N$  objects on the table. The final score for the table-cleaning task is calculated as follows:

$$S_{\text{clean}} = \frac{1}{N+2} (s_o + s_c + \sum_{i=1}^N s_i^d)$$

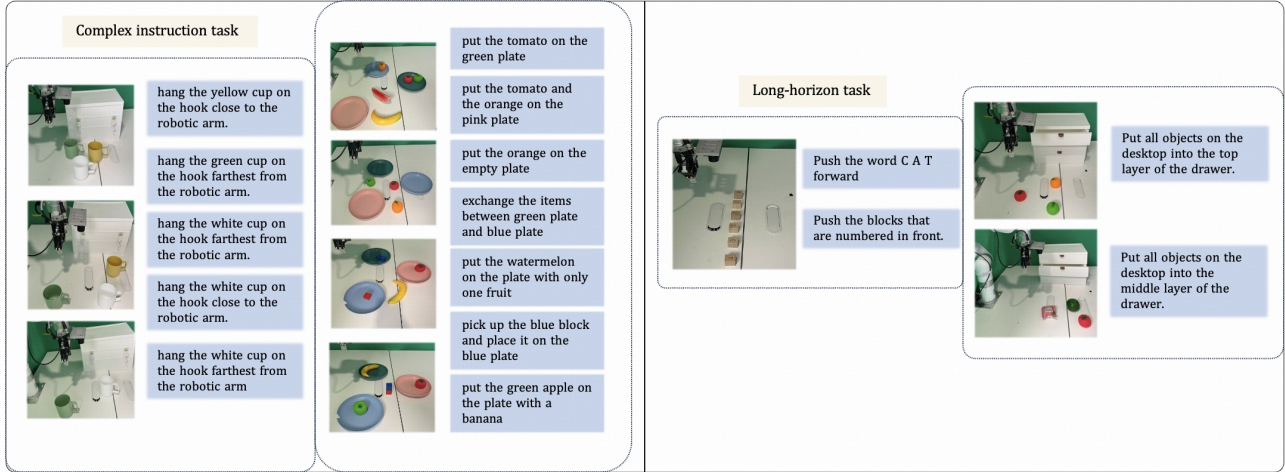


Figure 4. **Partial real machine environment and instruction diagram.** Our testing is based on the xArm robotic arm and DaHuan gripper. In real-world we collect 2000 trajectories and select for testing in this work.

- **Pick & Place:** In the pick-and-place task, the total score is comprised of a 60% completion component and a 40% accuracy component. The completion score  $s^d$  is awarded based on the successful grasping and placement of the  $N$  target objects specified in the instruction, following the same protocol as the table-cleaning task. The accuracy score  $s^r$  refers to the proportion of  $N$  correct objects identified by the model among a total of  $M$  objects. Notably, attempts are counted towards the accuracy score even if the grasp ultimately fails. we define score  $s \in \{0, 1\}$  based on whether the object is identified or not, For each object  $j$ , define  $r_j = 1$  if it is mentioned; define  $a_j=1$  if the agent attempts to grasp it at least once.

$$S_{\text{pick}} = 60\% \times \frac{1}{N} \sum_{i=1}^N s_i^d + 40\% \times \left(1 - \frac{1}{M} \sum_{j=1}^M [a_j \neq r_j]\right)$$

- **Hang Cups:** The “hang cups” task consists of two primary processes: picking up the cup and hanging the cup. To better evaluate the model’s sensitivity to instruction-specified orientations, we decompose the task into five sequential components: moving above the corresponding target  $s_m$ , successfully grasping the cup  $s_g$ , moving to the vicinity of the hook in the corresponding orientation  $s_h$ , aligning the cup handle with the hook  $s_a$ , and releasing the gripper to successfully hang the cup  $s_r$ :

$$S_{\text{cup}} = \frac{1}{5} \times (s_m + s_g + s_h + s_a + s_r)$$

### C. Task List of Real-World Tasks

We collected over 2,000 real-world trajectories involving more than 50 distinct objects in a physical robot environment. Notably, certain task configurations were excluded to serve as held-out scenarios for evaluation. For the Unseen tasks, neither the instructions nor the environments were present in the training set.

Our primary test environment is illustrated in Figure 4. The evaluation includes 34 distinct instruction types; to ensure representative results, some instructions were sampled multiple times in proportion to their natural frequency in the dataset.

#### C.1. Push Blocks Task

- Push the word C A T forward.
- Push the word G L M forward.
- Push the word D O G forward.
- Push the word V L A forward.
- Push the word R O S forward.

- Push the word I C E forward.
- Push the word Z H I P U forward.
- Push the word F L Y forward.
- Push the word L I K E forward.
- Push the word B O X forward.
- Push the blocks that are numbered in front.

### **C.2. Clean Table Task**

- Put all objects on the desktop into the top layer of the drawer.
- Put all objects on the desktop into the middle layer of the drawer.

### **C.3. Pick & Place Task**

- Put the tomato on the green plate.
- Put the tomato and the orange on the pink plate.
- Put the orange on the empty plate.
- exchange the items between the green plate and the blue plate.
- Put the green apple on the plate with a banana.
- Pick up the blue block and place it on the blue plate.
- Put the banana on the plate with two blue blocks.
- Put all items on the table into the pink plate.
- Put the orange on the plate with a red block.
- Put the watermelon on the plate with only one fruit.

### **C.4. Hang Cups Task**

- Hang the white cup on the hook farthest from the robotic arm.
- Hang the white cup on the hook close to the robotic arm.
- Hang the yellow cup on the hook close to the robotic arm.
- Hang the green cup on the hook farthest from the robotic arm.

### **C.5. Unseen Task**

- Exchange the position of the tomato and the pear.
- Put the tomato on the plate that has only one item of fruit.
- put as more as possible fruit to the green plate.
- Push the blocks with 7 multiplied by 6 forward.
- Push ahead the two blocks whose sum is over 14.
- Push the blocks that have numbers on them forward.
- Hang the green cup on the hook close to the robotic arm.
- Put all the blue blocks into the top layer of the drawer.

Table 12. Test results on the LIBERO dataset. “Model-FAST”: FAST tokenizer-assisted auto-regression model. “Model-Diffusion”: a VLM augmented with a diffusion action expert. “Model-ADV”: model incorporating VLM verification into model-Diffusion. Action chunk size per inference of our model is 16.

Models	Spatial	Object	Goal	Long	Avg.
Diffusion Policy (Chi et al., 2023)	78.3	92.5	68.3	50.5	72.4
HybridVLA (Liu et al., 2025)	93.6	90.6	90.2	84.4	90.2
FlowVLA (Zhong et al., 2025)	93.2	95.0	91.6	72.6	88.1
SmolVLA (Shukor et al., 2025)	93.0	94.0	91.0	77.0	88.8
OpenVLA-OFT (Kim et al., 2025a)	<u>97.6</u>	98.4	<b>97.9</b>	94.5	<u>97.1</u>
UniVLA (Bu et al., 2025)	95.4	<u>98.8</u>	93.6	94.0	95.5
Octo (Team et al., 2024)	78.9	85.7	84.6	51.1	75.1
OpenVLA (Kim et al., 2025b)	84.7	88.4	79.2	53.7	76.5
$\pi_0$ -FAST (Pertsch et al., 2025; Goyal et al., 2025)	90.0	86.0	95.0	73.0	86.0
VLA-0 (Lee et al., 2025)	94.4	97.6	93.0	90.6	93.9
GR00T-N1 (Bjorck et al., 2025)	94.4	97.6	93.0	90.6	93.9
$\pi_0$ (Black et al., 2025b)	96.8	<u>98.8</u>	95.8	85.2	94.2
$\pi_{0.5}$ -KI (Driess et al., 2025; Lee et al., 2025)	<b>98.0</b>	97.8	95.6	85.8	94.3
Discrete Diffusion VLA (Kim et al., 2025a)	97.2	98.6	<u>97.4</u>	92.0	96.3
Qwen2.5-VL-FAST	90.2	88.6	96.2	76.4	87.9
Qwen2.5-VL-Diffusion	94.6	97.2	93.8	90.2	93.9
<b>Qwen2.5-VL-ADV (Ours)</b>	96.6	<u>98.8</u>	97.0	<u>94.6</u>	96.8
InternVL3.5-FAST	89.6	92.8	93.6	82.8	89.6
InternVL3.5-Diffusion	95.8	96.0	94.2	92.8	94.7
<b>InternVL3.5-ADV (Ours)</b>	<u>97.6</u>	<b>99.4</b>	97.2	<b>96.8</b>	<b>97.8</b>

## D. Full Test Results on LIBERO and RoboTwin2.0

### D.1. LIBERO

**Settings.** For the LIBERO benchmark, we trained our model on 1,693 trajectories derived from data replay process (Kim et al., 2025b), and subsequently evaluated it on four tasks: Spatial, Object, Long, and Goal.

**Baselines.** In addition to auto-regressive baselines and diffusion VLAs, we compared our method against two main categories of models. First, we considered models that improve performance through inference framework modifications, such as Diffusion Policy, HybridVLA, VLA-0, and Discrete Diffusion VLA. Second, we included foundational models pre-trained on large-scale embodied datasets, such as RDT,  $\pi_0$ , GR00T-N1, and Octo.

For reference, we report published numbers for prior work when available in Table 12. Note that these results may differ in training data, action chunking, and evaluation protocol; our controlled comparisons are among Qwen / InternVL /  $\pi_{0.5}$  variants in Table 2 and Table 9. The results in Table 12 demonstrate that our method consistently outperforms the baselines across various objects. Notably, even without additional pre-training, our model achieves success rates comparable to those of large-scale pre-trained models on specific datasets. To further validate the effectiveness of the ADV framework, we also performed a series of ablation studies.

### D.2. RoboTwin 2.0

A partial selection of the RoboTwin test results is presented in the main body of the paper. For the full benchmark results of Qwen2.5-VL-Diffusion (Qwen-Dif) and Qwen2.5-VL-ADV (Qwen-ADV), please refer to Table 13.

Table 13. RoboTwin 2.0 Simulation Benchmark.

Simulation Task	RDT		Pi0		ACT		DP		Qwen-ADV		Qwen-Dif	
	Easy	Hard	Easy	Hard	Easy	Hard	Easy	Hard	Easy	Hard	Easy	Hard
<i>Adjust Bottle</i>	81%	<b>75%</b>	90%	56%	<b>97%</b>	23%	<b>97%</b>	0%	<b>97%</b>	26%	96%	16%
<i>Beat Block Hammer</i>	<b>77%</b>	<b>37%</b>	43%	21%	56%	3%	42%	0%	42%	0%	35%	0%
<i>Blocks Ranking RGB</i>	3%	0%	19%	5%	1%	0%	0%	0%	<b>52%</b>	<b>24%</b>	38%	11%
<i>Blocks Ranking Size</i>	0%	0%	7%	<b>1%</b>	0%	0%	1%	0%	<b>22%</b>	0%	16%	0%
<i>Click Alarmclock</i>	61%	12%	<b>63%</b>	11%	32%	4%	61%	5%	52%	<b>22%</b>	50%	19%
<i>Click Bell</i>	<b>80%</b>	9%	44%	3%	58%	3%	54%	0%	54%	<b>13%</b>	51%	12%
<i>Dump Bin Bigbin</i>	64%	<b>32%</b>	83%	24%	68%	1%	49%	0%	<b>77%</b>	15%	68%	21%
<i>Grab Roller</i>	74%	43%	96%	<b>80%</b>	94%	25%	<b>98%</b>	0%	78%	46%	66%	44%
<i>Handover Block</i>	45%	<b>14%</b>	45%	8%	42%	0%	10%	0%	<b>62%</b>	6%	54%	5%
<i>Handover Mic</i>	90%	<b>31%</b>	<b>98%</b>	13%	85%	0%	53%	0%	96%	2%	91%	4%
<i>Hanging Mug</i>	<b>23%</b>	<b>16%</b>	11%	3%	7%	0%	8%	0%	11%	0%	2%	0%
<i>Lift Pot</i>	72%	9%	84%	<b>36%</b>	88%	0%	39%	0%	<b>89%</b>	9%	82%	7%
<i>Move Can Pot</i>	25%	12%	<b>58%</b>	<b>21%</b>	22%	4%	39%	0%	56%	11%	48%	14%
<i>Move Pillbottle Pad</i>	8%	0%	<b>21%</b>	<b>1%</b>	0%	0%	1%	0%	17%	1%	<b>21%</b>	0%
<i>Move Playingcard Away</i>	43%	11%	<b>53%</b>	<b>22%</b>	36%	0%	47%	0%	50%	17%	48%	6%
<i>Move Stapler Pad</i>	<b>2%</b>	0%	0%	<b>2%</b>	0%	0%	1%	0%	0%	0%	0%	0%
<i>Open Laptop</i>	59%	32%	<b>85%</b>	<b>46%</b>	56%	0%	49%	0%	55%	27%	39%	18%
<i>Open Microwave</i>	37%	20%	80%	<b>50%</b>	<b>86%</b>	0%	5%	0%	62%	39%	55%	37%
<i>Pick Diverse Bottles</i>	2%	0%	<b>27%</b>	<b>6%</b>	7%	0%	6%	0%	21%	2%	22%	1%
<i>Pick Dual Bottles</i>	42%	<b>13%</b>	<b>57%</b>	12%	31%	0%	24%	0%	45%	9%	40%	5%
<i>Place A2B Left</i>	3%	<b>1%</b>	<b>31%</b>	<b>1%</b>	1%	0%	2%	0%	16%	0%	4%	0%
<i>Place A2B Right</i>	1%	1%	<b>27%</b>	<b>6%</b>	0%	0%	13%	0%	18%	0%	6%	1%
<i>Place Bread Basket</i>	10%	2%	17%	<b>4%</b>	6%	0%	14%	0%	<b>23%</b>	2%	11%	0%
<i>Place Bread Skillet</i>	5%	<b>1%</b>	<b>23%</b>	<b>1%</b>	7%	0%	11%	0%	9%	<b>1%</b>	8%	<b>1%</b>
<i>Place Burger Fries</i>	50%	<b>27%</b>	<b>80%</b>	4%	49%	0%	72%	0%	68%	11%	45%	2%
<i>Place Can Basket</i>	19%	<b>6%</b>	<b>41%</b>	5%	1%	0%	18%	0%	21%	2%	15%	3%
<i>Place Cans Plasticbox</i>	6%	<b>5%</b>	34%	2%	16%	0%	<b>40%</b>	0%	11%	0%	14%	0%
<i>Place Container Plate</i>	78%	17%	<b>88%</b>	<b>45%</b>	72%	1%	41%	0%	82%	11%	68%	2%
<i>Place Dual Shoes</i>	4%	<b>4%</b>	<b>15%</b>	0%	9%	0%	8%	0%	12%	0%	8%	0%
<i>Place Empty Cup</i>	56%	7%	37%	<b>11%</b>	<b>61%</b>	0%	37%	0%	44%	3%	37%	0%
<i>Place Fan</i>	12%	2%	<b>20%</b>	<b>10%</b>	1%	0%	3%	0%	4%	1%	2%	0%
<i>Place Mouse Pad</i>	1%	0%	<b>7%</b>	<b>1%</b>	0%	0%	0%	0%	0%	0%	1%	0%
<i>Place Object Basket</i>	<b>33%</b>	<b>17%</b>	16%	2%	15%	0%	15%	0%	22%	4%	14%	1%
<i>Place Object Scale</i>	1%	<b>0%</b>	<b>10%</b>	<b>0%</b>	0%	<b>0%</b>	1%	<b>0%</b>	0%	<b>0%</b>	0%	<b>0%</b>
<i>Place Object Stand</i>	15%	5%	<b>36%</b>	<b>11%</b>	1%	0%	22%	0%	9%	0%	11%	0%
<i>Place Phone Stand</i>	15%	6%	<b>35%</b>	<b>7%</b>	2%	0%	13%	0%	17%	6%	11%	2%
<i>Place Shoe</i>	<b>35%</b>	<b>7%</b>	28%	6%	5%	0%	23%	0%	24%	2%	16%	0%
<i>Press Stapler</i>	41%	24%	<b>62%</b>	<b>29%</b>	31%	6%	6%	0%	55%	15%	44%	7%
<i>Put Bottles Dustbin</i>	21%	4%	<b>54%</b>	<b>13%</b>	27%	1%	22%	0%	28%	9%	14%	6%
<i>Put Object Cabinet</i>	33%	<b>18%</b>	<b>68%</b>	<b>18%</b>	15%	0%	42%	0%	55%	0%	42%	0%
<i>Rotate QRcode</i>	50%	5%	<b>68%</b>	<b>15%</b>	1%	0%	13%	0%	35%	9%	26%	12%
<i>Scan Object</i>	4%	<b>1%</b>	<b>18%</b>	<b>1%</b>	2%	0%	9%	0%	11%	0%	9%	0%
<i>Shake Bottle Horizontally</i>	84%	<b>51%</b>	<b>99%</b>	<b>51%</b>	63%	4%	59%	18%	87%	42%	83%	19%
<i>Shake Bottle</i>	74%	45%	<b>97%</b>	<b>60%</b>	74%	10%	65%	8%	86%	37%	84%	21%
<i>Stack Blocks Three</i>	2%	<b>0%</b>	<b>17%</b>	<b>0%</b>	0%	<b>0%</b>	0%	<b>0%</b>	2%	<b>0%</b>	0%	0%
<i>Stack Blocks Two</i>	21%	<b>2%</b>	<b>42%</b>	1%	25%	0%	7%	0%	17%	<b>2%</b>	18%	1%
<i>Stack Bowls Three</i>	51%	17%	<b>66%</b>	24%	48%	0%	63%	0%	61%	<b>26%</b>	52%	9%
<i>Stack Bowls Two</i>	76%	30%	<b>91%</b>	41%	82%	0%	61%	0%	84%	<b>48%</b>	75%	24%
<i>Stamp Seal</i>	1%	0%	3%	<b>4%</b>	2%	0%	2%	0%	<b>4%</b>	0%	0%	0%
<i>Turn Switch</i>	35%	15%	27%	<b>23%</b>	5%	2%	<b>36%</b>	1%	22%	9%	15%	7%
<i>Average (%)</i>	34.5	<u>13.7</u>	<b>46.4</b>	<b>16.3</b>	29.7	1.7	28.0	0.6	<u>39.3</u>	10.2	30.1	6.7